

Effect of Electrolytic Conditions on Electrodeposition of Manganese in NaCl-KCl Melt

Guolong Liu^{1,2}, Wei Liu^{1,2}, Qian Kou^{1,2}, Sajun Xiao^{1,2,*}

¹ School of Metallurgy Engineering, Anhui University of Technology, Maanshan, Anhui, China, 243002;

² Key Laboratory of Metallurgical Emission Reduction & Resources Recycling, Anhui University of Technology, Maanshan, Anhui, China, 243002

*E-mail: xiaosajunzj@yahoo.com

Received: 15 November 2017 / Accepted: 14 January 2018 / Published: 5 February 2018

In this paper, molten NaCl-KCl-MnCl₂ mixture salts were used as electrolyte, tungsten as the cathode and graphite as the anode to explore the influence of different current density, electrolysis temperature and electrolysis time on current efficiency and microstructure of manganese deposits. The morphology of products were examined by scanning electron microscopy. The results demonstrated that the current efficiency and morphology of deposited manganese varied with electrodeposition time, operating temperature and current density. The optimized conditions for the highest current efficiency (98%) were obtained at the temperature of 710°C, with the electrodeposition time for 7h and the operating current density of 300 mA • cm⁻², respectively.

Keywords: Manganese, Electrodeposition, Molten salts, Current efficiency, Morphology

1. INTRODUCTION

Manganese is an important alloy element and always used to complete the preparation of different types of steels [1-3]. The addition of Mn to steels not only improves its strength and stiffness but also enhances its corrosion resistance and metal elasticity [4]. In fact, the study about the production of manganese and its alloys via electrolysis technology has been carried out for past several decades because of its electronegative characteristic [5-9]. Recently, considerable attention was attracted in the manufacture of metal manganese for the development of high manganese and high strength automotive steel, which contains a content of manganese up to 10-30% (wt) [10-11].

High manganese (10-30% (wt)) and high strength steel can lead to light-weight and improvement of the safety of the car, which requires high-purity and low-cost ferromanganese as the

Mn-bearing alloy agent. The feeding manganese into this type of steel is mainly from electrolytic manganese, which is expensive because of high cell voltage and low current efficiency in present process. Besides, a shortage of raw material MnCO_3 ore for electrolytic manganese also increased its cost [12]. Therefore, it attracted much attention for how to prepare low-cost and high-purity manganese or ferromanganese. Selecká and Šalak [13], in their study of electrolytic manganese and the powder grades of ferromanganese, described the main characteristics of electrolytic manganese and of high carbon and medium carbon ferromanganese. Safarian and his coworkers [14] has reported the purity requirements for Mn alloys for manufacturing high manganese TRIP and TWIP steels, and Hils [15] also had a similar discussion. Xiao group [16-17] studied the electrochemical behavior of manganese ion in molten NaCl-KCl and reported the preparation of refined pure ferromanganese from high carbon ferromanganese using the same molten salts electrolyte. However, investigation on the effects of experimental parameters on the microstructures and current efficiency of electrodeposits has not been carried out.

Based on previous investigation [16], we mainly focus on the discussion of the influence of different process parameters such as current density, electrolysis temperature and electrolysis time on current efficiency and microstructure of manganese deposits in NaCl-KCl-MnCl_2 (2%(wt)) system, to provide support for subsequent investigation on optimization of refining process to produce high-purity manganese or ferromanganese from high carbon ferromanganese.

2. EXPERIMENTAL

2.1 Experimental apparatus and electrodes

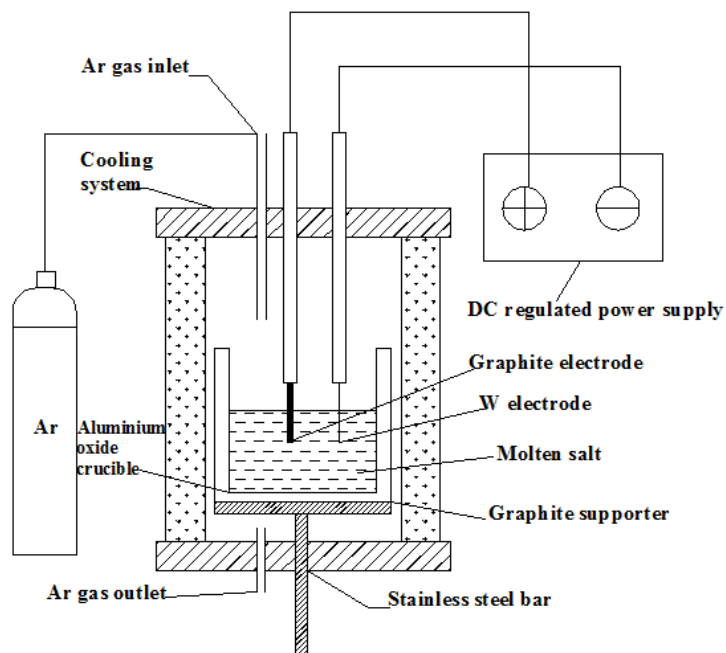


Figure 1. Schematic of the experimental set-up.

The experimental apparatus for electrodeposition of manganese in this study is given schematically in Figure1. Alumina crucible was employed as electrolytic cell which was supported by a graphite supporter. The crucible was introduced into an alumina tube which was closed by stainless sealed lids cooled by circulating water and positioned by a programmable vertical furnace. And the furnace also provide the heat required to maintain a constant temperature in the experiment. A graphite rod of 8mm diameter connected with a stainless steel rod acting as the current lead was employed as the anode. A tungsten wire with a diameter of 1 mm shielded with a thin corundum tube was selected as the cathode, which was dipped into the melt with a depth of about 10mm. Before immersed into electrolyte, the two electrodes were polished with fine emery paper and washed with ethanol. The electrolysis was conducted with an equipment of DLCC5000L DC regulated power source. During the electrolysis, an argon atmosphere was provided inside the furnace tube.

2.2 Preparation of electrolyte

All reagents in this experiment are NaCl, KCl, and MnCl₂, all of them are analytic grade. NaCl and KCl were dried at a temperature of 200°C in drying oven for more than 48h to remove surface water. Afterwards, an equimolar NaCl-KCl was employed as the supporting electrolyte and MnCl₂ were mixed evenly. The content of MnCl₂ was 2% (wt).

2.3 Electrolysis and analysis of deposits

Electrodeposition was conducted under various experimental conditions such as current density, electrolytic temperature and electrolytic time. After electrolysis, the deposits on the cathode as well as in the melt were collected. The specimens collected were washed with distilled water, followed with acetone, and dried in vacuum drying oven. The obtained products were analyzed by scanning electron microscopy (SEM).

The current efficiency η was computed using the equation (1) as follows:

$$\eta = \frac{Q_c}{Q_a} \times 100\% \quad (1)$$

$$Q_c = \frac{m}{M} \times nF \quad (2)$$

Where Q_c and Q_a (C) are the quantity of transferred electric charge calculated by the actual weight of the product and total electric charge during electrodeposition process, respectively, m (g) is the mass of the deposited manganese, M (g/mol) is the molar mass of manganese, n is the number of transferred electron and F is the Faraday constant.

3. RESULTS AND DISCUSSION

3.1 Effect of current density

The effect of current density during electrolysis on the cathode current efficiency and the morphology of electrodeposited manganese was investigated. The relationship between current density

and cathode current efficiency at a constant temperature (710°C) and time (5h) is shown in Fig.2. Cathode current efficiency is calculated according to the ratio of weight of the products collected from the cathode and the molten salts and the theoretical weight based on the Faraday formula. It can be seen clearly from Fig.2 that the current efficiency shows a decreasing tendency as the current density increases. In addition, it can be observed from Fig.3 that manganese particles become smaller with the increase of current density. Since higher current density results in the presence of finer powder in products, the obtained products are mixed with molten salts more easily, resulting in more loss of products during the recovery process. Therefore, the current efficiency decreases with the rise of current density. Lei and Sullivan [18] applied lower cathode current on the electrolytic cell to extract vanadium from V_2C in a $\text{BaCl}_2\text{-KCl-NaCl-VCl}_2$ electrolyte, resulting in coarser particle, low electrolyte dragout with deposits and good cathode current efficiencies. Xu group [19] also reported the similar results in the study of the current efficiency of recycling aluminum from aluminum scraps by electrolysis in $\text{AlCl}_3\text{-NaCl}$ molten salts.

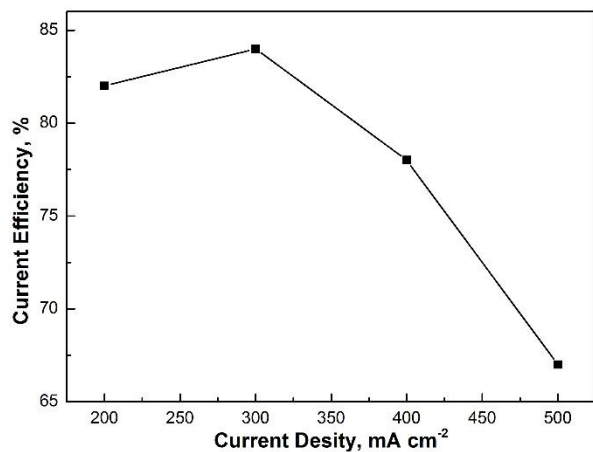


Figure 2. Effect of different current density ($200 \text{ mA} \cdot \text{cm}^{-2}$; $300 \text{ mA} \cdot \text{cm}^{-2}$; $400 \text{ mA} \cdot \text{cm}^{-2}$; $500 \text{ mA} \cdot \text{cm}^{-2}$) on current efficiency at 710°C for 5h.

Fig.3 displays the SEM micrographs of manganese deposits at different current density. Fig.3 (a) gives the microstructure of manganese electrodeposited at the lowest current density ($200 \text{ mA} \cdot \text{cm}^{-2}$), which shows relatively uniform spherical particles, and most of them have a particle size distribution between $50\mu\text{m}$ and $80\mu\text{m}$. Fig.3 (b) depicts the microstructure of the deposited manganese prepared at the current density of $300 \text{ mA} \cdot \text{cm}^{-2}$. Intuitively, the microstructure observed in this picture is similar to that in Fig.3 (a), but its particles size is smaller. At a slightly higher current density ($400 \text{ mA} \cdot \text{cm}^{-2}$), the deposited manganese particles become finer than that in (a) and (b), and there are some amount of agglomeration of particles present. The electron microscope picture of the deposit obtained at $500 \text{ mA} \cdot \text{cm}^{-2}$ given in Fig.3 (d) shows a non-uniform deposit morphology, which not only contains fine spherical particles, but also contains dendritic structure. In fact, according to author's previous work [16], it can be known that the reduction process of Mn (II) on W electrode is a quasi-reversible reaction controlled by diffusion. So the deposits often tend to form dendrites at high current density [18]. According to the formula (3) [20], the crystal nucleation number increases with the rise of

current density, which results in the existence of large amount of finer particles. High current densities cause serious polarization and high overpotential, thus the nucleating current density is larger than growing current density. The deposits tend to form fine powder. Therefore, in Fig. 3 the particle size of the deposited manganese becomes smaller as the current density increases. Actually, in the studies of preparation of high purity titanium powder by molten salt electrolysis, the same trend was observed by a large amount of investigators [21-24].

$$N_n = a + b \times \lg[D_k/C_{me}] \quad (3)$$

Where N_n is crystal nucleation number, a, b are constants related to the properties of the metal, D_k is cathode current density and C_{me} is the concentration of manganese ions in molten salts.

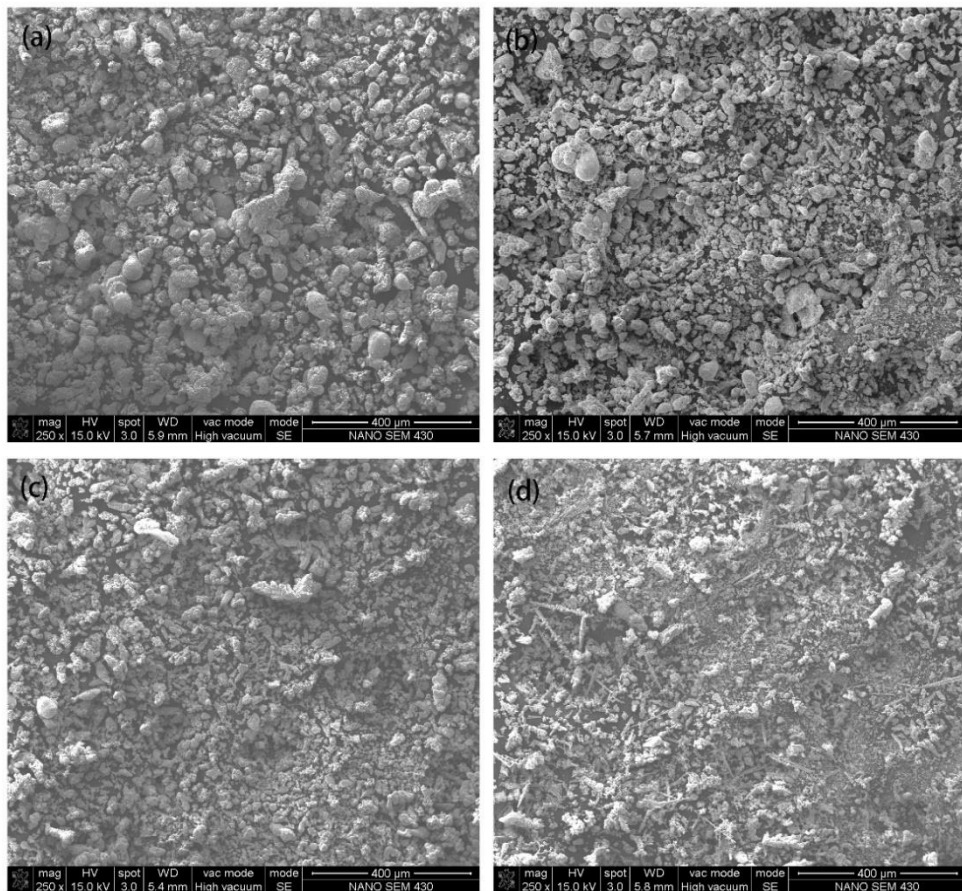


Figure 3. SEM micrographs of manganese deposits in different current density at 710°C for 5h : (a) 200 $\text{mA} \cdot \text{cm}^{-2}$; (b) 300 $\text{mA} \cdot \text{cm}^{-2}$; (c) 400 $\text{mA} \cdot \text{cm}^{-2}$; (d) 500 $\text{mA} \cdot \text{cm}^{-2}$.

3.2 Effect of different temperature

Current efficiency of the manganese electrodeposition is not only affected by current density, but also influenced by temperature. As presented in Fig.4, the current efficiency drops approximately linearly with the increase of electrolysis temperature from 710°C to 860°C.

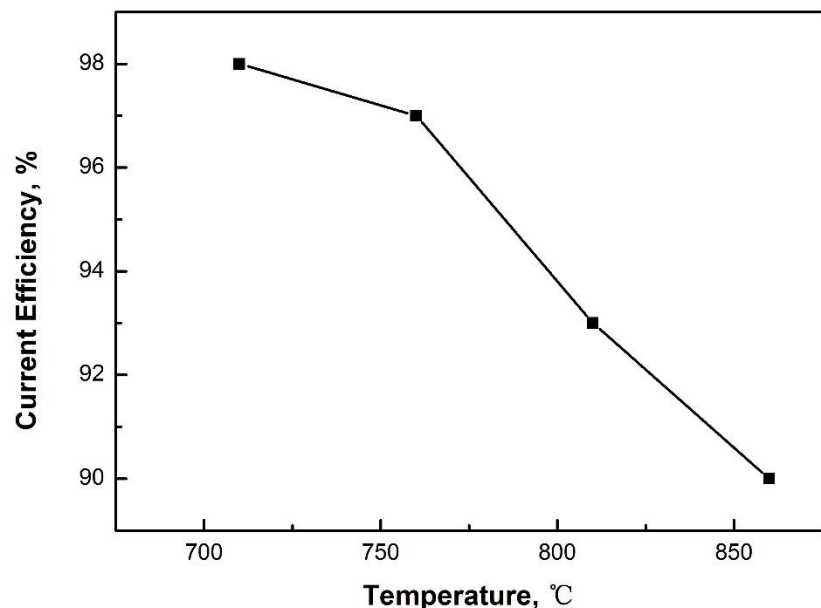


Figure 4. Effect of different temperature (710°C ; 760°C ; 810°C ; 860°C) on current efficiency at $300 \text{ mA} \cdot \text{cm}^{-2}$ for 5h.

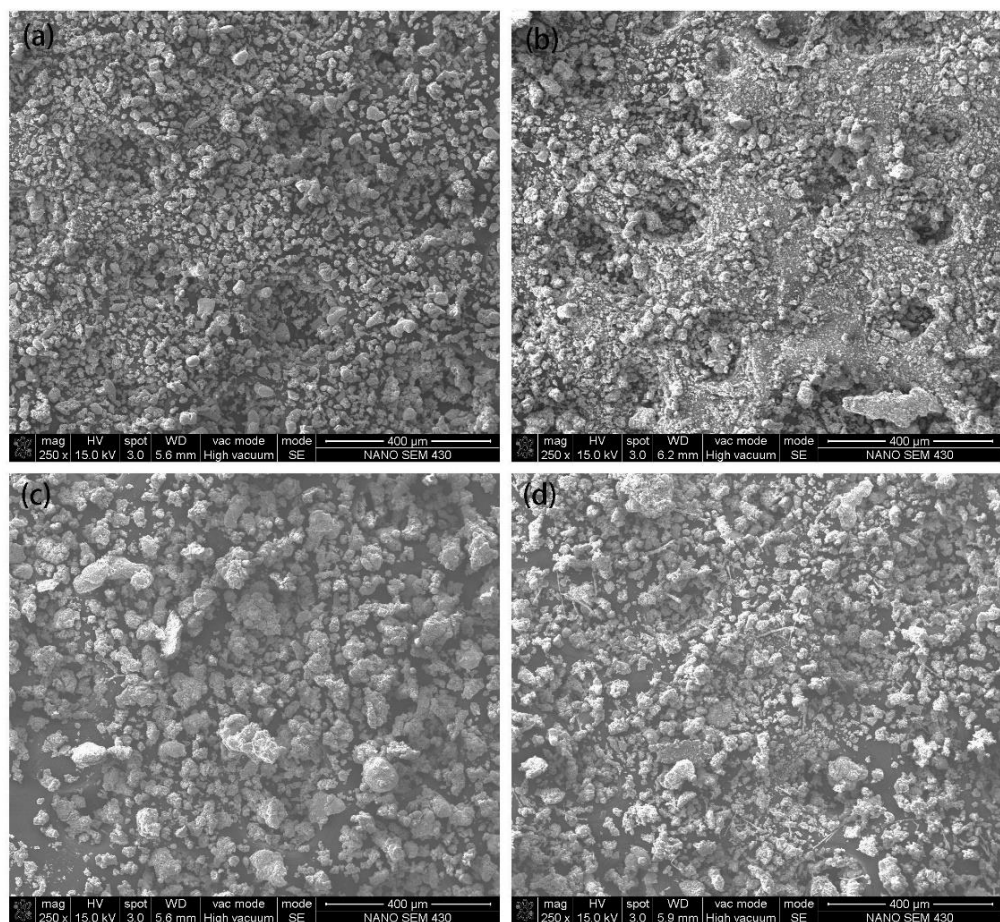


Figure 5. SEM micrographs of manganese deposits in different temperature at $300 \text{ mA} \cdot \text{cm}^{-2}$ for 5h.: (a) 710°C ; (b) 760°C ; (c) 810°C ; (d) 860°C .

This is because the increase of temperature exacerbates the volatilization of electrolyte, resulting in the instability of the electrolysis process. In addition, the increase of temperature leads to an increase in the solubility of the electrodeposited manganese in the electrolyte and accelerate the pace of diffusion of the cathode product, thereby increase the loss of products and reduce current efficiency. This has been confirmed extensively for the aluminum electrolysis in molten cryolite-based melt [25].

In practice, the electrolysis temperature should not be too low, because the low temperature increases the viscosity of the electrolyte, which results in more physical loss of the deposits. Therefore, it is necessary to carry out some tests to find the most favorable electrolytic conditions to lower the electrolysis temperature while maintaining good electrolyte mobility.

The SEM micrographs of the electrodeposited manganese at different electrolysis temperature are given in Fig.5. Overall, all deposits prepared at the temperature range from 710°C to 860°C show a granular microstructure, but only the products obtained at 710°C are found more uniform with the average size from 20 µm to 40 µm. At 760°C, the deposits show a mixture of large particles and small particles, and the fine powder products occupy a large proportion. At higher temperature (over 800°C), there are some aggregated particles present. In principle, the particle size should be bigger with the increase of temperature due to acceleration of diffusion and decrease of the overpotential of deposition of metal ions. Wei and Weng [26-27] presented the similar findings in their studies of electroplating of titanium and preparation of titanium in molten salts. Although the particle size does not changes according to this principle in Fig 5, larger particles at a higher temperature (810°C) were also observed.

3.3 Effect of electrodeposition time

The effect of electrodeposition time on the cathode current efficiency and morphology of electrodeposited manganese were analyzed at the time range from 5h to 8h at constant current density ($200 \text{ mA} \cdot \text{cm}^{-2}$) and constant temperature (710°C). Fig.6 describes the variation of electrolysis time with current efficiency. It can be observed that as the electrolysis time increases the current efficiency increases first and then decreases. The current efficiency reaches its maximum value (98%) when the electrolysis time prolongs to 7h. But when electrodeposition time continue to increase to 8h, the current efficiency decrease to 85%, which can be explained by the SEM images (Fig.7). The products prepared at the electrodeposition time of 7h appears much finer, causing much loss of cathode products during collection process, which may act as the main influence factor for current efficiency in this case.

The SEM micrographs of manganese deposits at different electrolysis time are shown in Fig.7. As can be seen clearly, the longer electrodeposition time results in the decrease of powder particles. Especially in Fig.7(d), most of the deposits are powdered. Generally, the particles on the cathode should grow bigger and bigger with the increasing time. However, in our experiment most of the formed cathode products did not attach on the surface of cathode and fell into the melt. Thus, the main influence on the products particle size is the concentration of manganese ions.

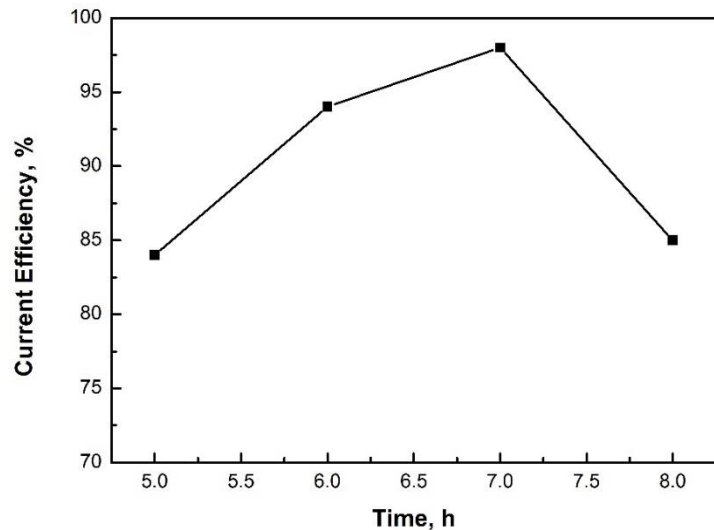


Figure 6. Effect of different electrodeposition time (5 h; 6 h; 7 h; 8 h) on current efficiency in $300 \text{ mA} \cdot \text{cm}^{-2}$ at 710°C .

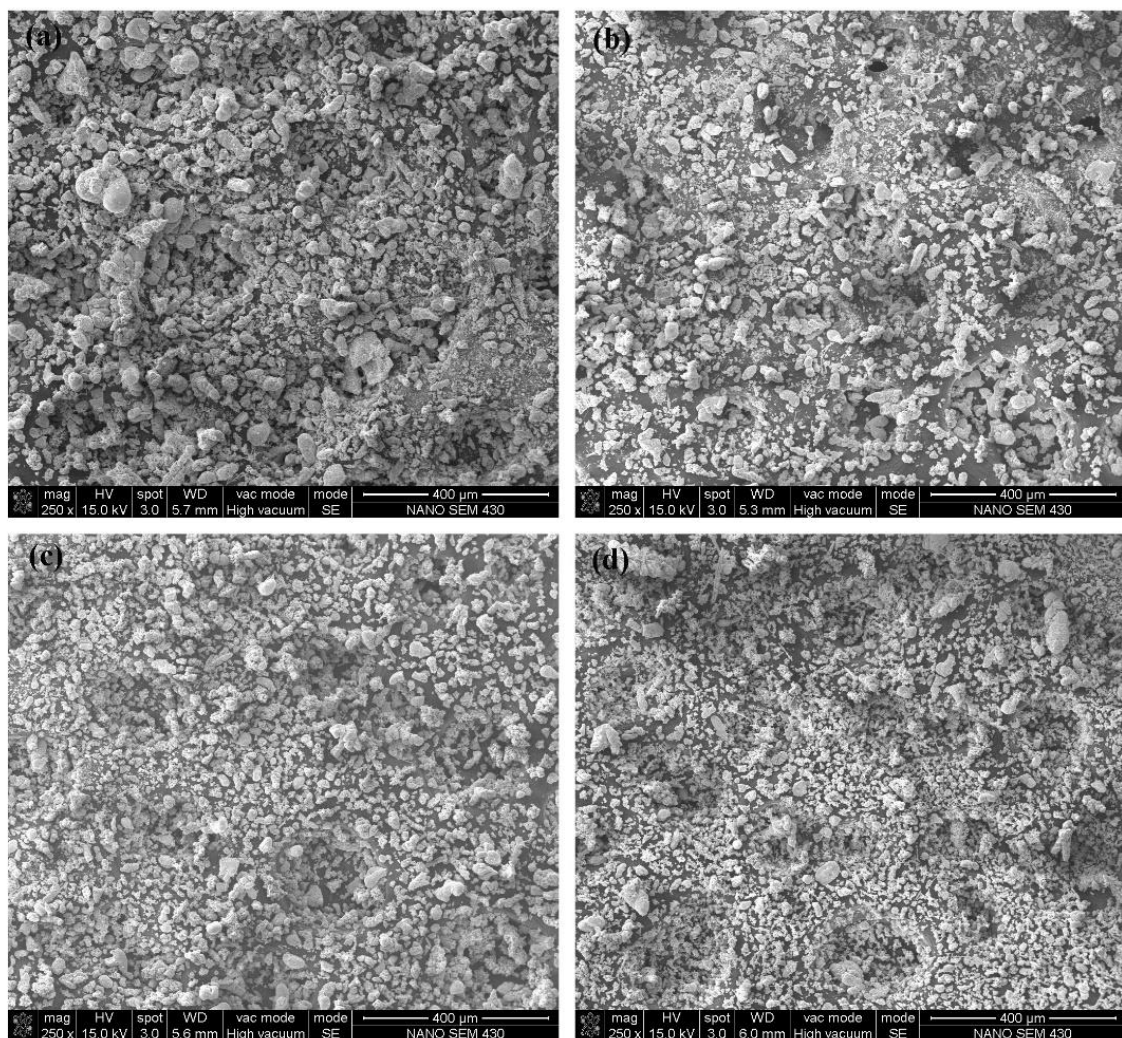


Figure 7. SEM micrographs of manganese deposits at different electrolysis time in $300 \text{ mA} \cdot \text{cm}^{-2}$ at 710°C : (a) 5 h; (b) 6 h; (c) 7 h; (d) 8 h.

Actually, during the electrolysis, the concentration of manganese ions in the melt decreased gradually. Therefore, from the formula (3), it can be found that the decrease of the concentration of manganese ions in molten salts results in a larger number of nuclei (N_n), which leads to finer powder present. Actually, the low concentration results in concentration polarization and high overpotential. Thus the crystal nucleating current density is bigger than growing current density, and the growth of the crystal is hindered, leading to much existence of nuclei without growing. Meanwhile, polarization results in a thick diffusion layer and nonuniform growth of the deposits on the electrode surface, causing formation of loose and fine powder. Liu and Weng [23-24] demonstrated the similar trend in their studies of deposition of titanium in $\text{NaCl}-\text{KCl}-\text{TiCl}_x$ electrolyte.

4. CONCLUSIONS

The influence of different current density, electrolysis temperature and electrolysis time on current efficiency and microstructure was investigated in $\text{NaCl}-\text{KCl}-\text{MnCl}_2$ system. It was found that the current efficiency and morphology of electrodeposits vary with different experimental parameters. The detailed results from present investigation are as follows:

(1) Current density has a significant effect on the morphology of manganese deposits. With the increase of current density, the particle size of electrolytic products showed a decreasing trend. The current efficiency is also significantly affected by current density, temperature and electrolysis time.

(2) The highest current efficiency (98%) were achieved at the temperature of 710°C, with the electrodeposition time for 7 h and the operating current density of $300 \text{ mA} \cdot \text{cm}^{-2}$.

ACKNOWLEDGEMENTS

The authors are grateful for the financial support from National Natural Science Foundation of China, Project (51404001) and Anhui Province overseas scholars innovation project funding program.

References

1. P. Ilea, I. C. Popescu, M. Urdă, L. Oniciu, *Hydrometallurgy*, 46 (1997) 149.
2. R. S. Dean, Electrolytic manganese and its alloys, (1952)Ronald Press Co, U. S.
3. J. H. Tan, H. Y. Chen, S. T. Zhang, Q. Xiang, *Adv. Mate. Res.*, 194 (2011) 275.
4. J. Lu, D. Dreisinger, T. Glück, *Hydrometallurgy*, 141 (2014) 105.
5. H. H. Oaks, W. E. Bradt, *J. Electrochem. Soc.*, 69 (1936) 567.
6. J. H. Jacobs, P. E. Churchward, *J. Electrochem. Soc.*, 94 (1948) 108.
7. M. A. Qazi, J. Leja, *J. Electrochem. Soc.*, 118 (1971) 548.
8. M. Gonsalves, D. Pletcher, *J. eletroanal. chem.*, 285 (1990) 185.
9. P. Díaz-Arista, R. Antaño-López, Y. Meas, R. Ortega, E. Chainet, P. Ozil, G. Trejo, *Electrochim Acta*, 51 (2006) 4393.
10. O. Grässel, L. Krüger, G. Frommeyer, L. M. Meyer, *Int. J. Plasticity*, 16 (2000) 1391.
11. D. Barbier, N. Gey, S. Allain, N. Bozzolo, M. Humbert, *Matre. Sci. Eng.*, 500 (2009) 196.
12. J. Lu, D. Dreisinger, T. Glück, *Hydrometallurgy*, 141 (2014) 105.
13. M. Selecka, A. Šalak, *Powder. Metall. Prog.*, 9 (2009) 97.

14. J. Safarian, L. Kolbeinsen, Purity requirements for Mn alloys for producing high manganese trip and twip steels, Infacon XIII, (2013) Almaty, Kazakhstan.
15. G. Hils, A. Newirkowez, M. Kroker, U. Grethe, S. J. Rune, J. Kroos, K. H. Spitzer, *Steel. Res. Int.*, 86 (2015) 411.
16. S. Xiao, W. Liu, L. Gao, *Ionics*, 22 (2016) 2387.
17. S. Xiao, W. Liu, L. Gao, J. Zhang, *Arch. Metall. Mater.*, 62 (2017) 1505.
18. K. P. V. Lei, T. A. Sullivan, Electrolytic preparation of vanadium from V₂C-type Carbide, (1971) Bureau of Mines, U. S. Hong. Li, Metallurgical principle, (2005) Science Press, Beijing.
19. J. Xu, J. Zhang, Z. Shi, B. Gao, Z. Wang, X. Hu, *Trans. Nonferrous. Met. Soc. China.*, 24 (2014) 250
20. H. Li, Metallurgical principle, (2005) Science press, Beijing.
21. N. Guo, Y. Gao, C. Wang, *Rare. Metals.*, 02 (1983) 14.
22. F. Zhu, K. Qiu, C. Sun, T. Mu, B. Deng, *Iron. Steel. Vanadium. Titanium.*, 38 (2017)
23. H. Liu, N. Sun, X. Ning, H. Zhu, *J. Rare. Earths.*, 28 (2010) 177.
24. Q. Weng, Z. Zhou, H. Lin, J. Yuan, T. Yuan, *Mat. Sci. Eng. Pow. Metall.*, 1 (2010) 70.
25. J. Thonstad, P. Fellner, G. M. Haarberg, J. Híveš, H. Kvande, Á. Sterten, Aluminium electrolysis fundamentals of the hall-héroult process, (2001) Aluminium Verlag Marking & Kommunikation GmbH, Germany.
26. D. Wei, M. Okido, T. Oki, *J. Appl. Electrochem.*, 24 (1994) 923.
27. Q. Weng, R. Li, T. Yuan, J. Li, Y. He, *Trans. Nonferrous. Met. Soc. China.*, 24 (2014) 553.

© 2018 The Authors. Published by ESG (www.electrochemsci.org). This article is an open access article distributed under the terms and conditions of the Creative Commons Attribution license (<http://creativecommons.org/licenses/by/4.0/>).